Evaluating Spatial Details of Luojia-1 Night-Time Images Using Road Network Analysis

Huimin Xu[1] and Xi Li[2](✉)

[1] Economics School, Wuhan Donghu University, Wuhan 430212, China
[2] State Key Laboratory of Information Engineering in Surveying, Mapping and Remote Sensing, Wuhan University, Wuhan 430079, China
li_rs@163.com

Abstract. Luojia-1 satellite is a new launched night-time light satellite providing 130 m resolution images. To evaluate the additional spatial details of Luojia-1 compared to VIIRS images, we employed road network analysis to compare the two kinds of images in Los Angeles, United States. In the road network analysis, we calculated the correlation coefficients between the distance to the primary road and the image radiance in 228 neighborhood areas, and we found that the average Spearman correlation coefficient is −0.3843 for Luojia-1 and −0.0974 for VIIRS, while those of the Pearson correlation coefficients are −0.3129 and −0.1370, respectively. In addition, we also calculated the Pearson correlation coefficients between the distance to the road intersections and the image radiance, and the average coefficient for Luojia-1 is −0.2967 and that of the VIIRS is −0.1100. The road network analysis suggests that the night-time light radiance in Luojia-1 is stronger correlated to the road network than VIIRS. All these findings show that Luojia-1 images provide richer information to reflect urban structures than VIIRS, indicating that Luojia-1 images have potential for studying urban socioeconomic parameters at a fine resolution.

Keywords: Night-time light · Luojia-1 · VIIRS · Spatial resolution · Road network

1 Introduction

In 1970s, the Defense Meteorological Satellite Program's Operational Linescan System (DMSP/OLS) had been proved effective to detect night-time light from oil fields [1] and human settlements [2]. Since then, the DMSP/OLS night-time light images had been widely applied in estimating energy consumption [3] and Gross Domestic Product (GDP) [4] as well as mapping population density [5] and urban extent [6, 7]. In 2011, the National Geophysical Data Center (NGDC) has released a time series dataset of DMSP/OLS image, and updated the dataset to 1992–2013. Since then, time series analysis of DMSP/OLS images have been employed for studies of urbanization [8–10], economic growth [11], humanitarian disasters [12] and light pollution [13]. Although NGDC provided time series DMSP/OLS between 1992 and 2013, it has stopped to update the recent products. Furthermore, the DMSP/OLS is lacking of

Y. Xie et al. (Eds.): GSES 2019/GeoAI 2019, CCIS 1228, pp. 122–131, 2020.
https://doi.org/10.1007/978-981-15-6106-1_9

on-board radiometric calibration, and the spatial resolution is only 2.7 km. These problems have limited the usage of DMSP/OLS. In the end of 2011, the launch of Suomi National Polar-orbiting Partnership satellite's Visible Infrared Imaging Radiometer Suite (Suomi NPP/VIIRS) is a new milestone for the night-time light community. The day and night band (DNB) on VIIRS provides wide radiometric range and spatial resolution of 742 m, which are better than DMSP/OLS [14] and are able to provide rich information to model urban structures [15].

On June 2, 2018, at Jiuquan Satellite Launch Center, China's Wuhan University launched Luojia-1 01 satellite (abbreviated as Luojia-1 in the rest of this paper), which is a small satellite in 20 kg weight. One purpose of the satellite is to provide free global night-time light images at a finer resolution than VIIRS DNB. The spatial resolution of Luojia-1 is 130 m, with the local visiting time close to 9:30 PM. Luojia-1 satellite has a panchromatic band with wavelength between 460 nm–980 nm, which is wider than the VIIRS DNB wavelength (e.g. 500 nm–900 nm). The Luojia-1 data is now open to global users at Hubei Data and Application Network for High Resolution Earth Observation System (http://59.175.109.173:8888/app/login_en.html). A number of studies have been done to investigate the potential of Luojia-1 and its applications [16, 17], few analysis has been taken to explore the spatial information of Luojia-1 images. Although a previous study shows the Luojia-1 image has more spatial details than VIIRS based on the wavelet analysis [16], a more physical analysis is still needed to compare the two kinds of images. This paper aims to evaluate the spatial information provided by the Luojia-1 image, by comparing it with a VIIRS night-time light image, using road network analysis.

2 Materials and Methods

2.1 Data and Study Area

The study area is Los Angeles, the United States. The study data includes administrative boundaries, night-time light images and road network data. The administrative boundaries were downloaded from Los Angeles County Enterprise GIS (https://egis3.lacounty.gov/eGIS/) and shown in Fig. 1. The full dataset includes 272 neighborhood areas, and 265 neighborhood areas were extracted in this research since the rest of areas is not overlapped or only partly overlapped with the Luojia-1 image. However, some neighborhood areas in the 265 neighborhood areas will be discarded in part of this study because of sample size. The night-time light images include both Luojia-1 image and VIIRS images for Los Angeles. A Luojia-1 image (Fig. 2), which was captured on June 6, 2018, was downloaded from Hubei Data and Application Network for High Resolution Earth Observation System. The VIIRS image (Fig. 3) was extracted from monthly average composite for May 2018, downloaded from the National Geophysical Data Center (NGDC). The road network data for Los Angeles was downloaded from the Open Street Map (https://www.openstreetmap.org/).

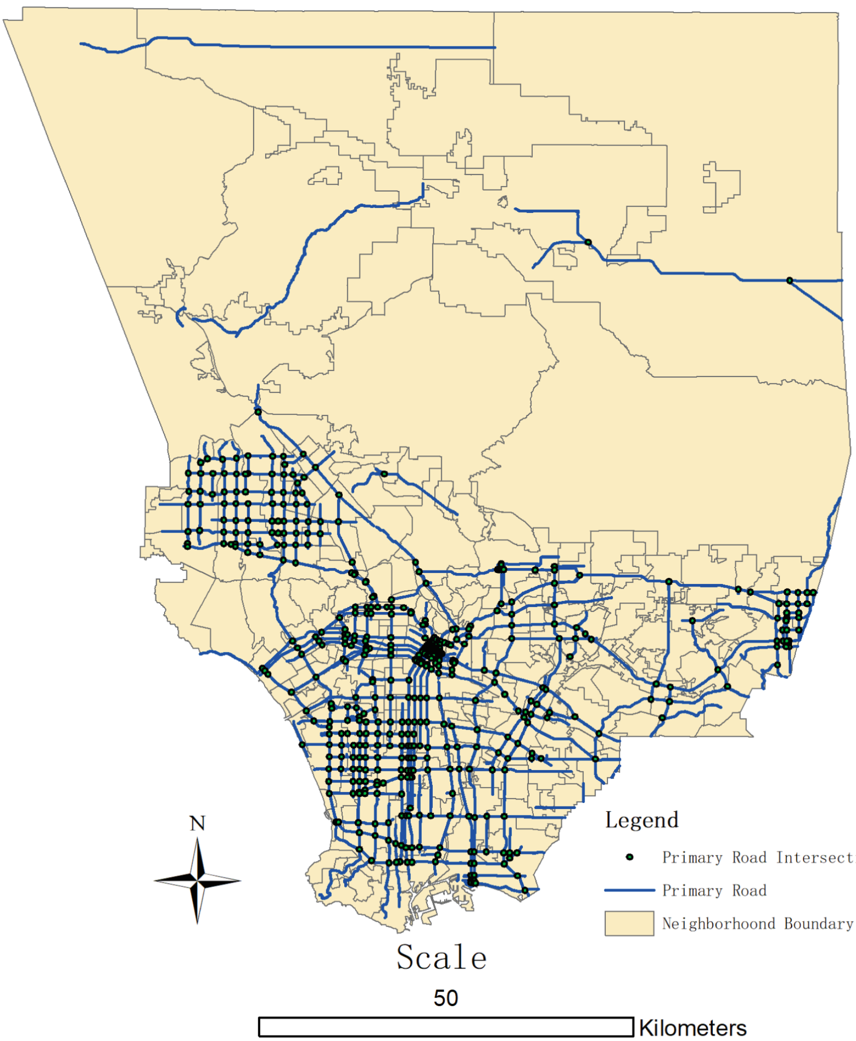

Fig. 1. The 265 neighborhood areas, primary roads and primary road intersections in Los Angeles, United States.

2.2 Preprocessing Data

All the geographic data were projected into coordinate system of WGS_1984_UTM_Zone_11N. For the Luojia-1 image and VIIRS image, they were resampled into 100 m resolution with bilinear spatial interpolation. For the Luojia-1 image, all the digital numbers (DNs) were transformed into radiance.

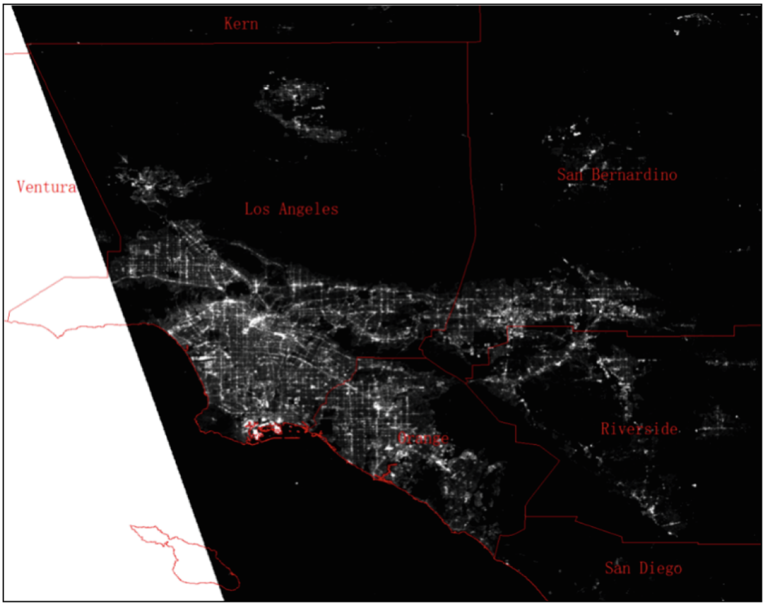

Fig. 2. Luojia-1 night-time light image for Los Angeles

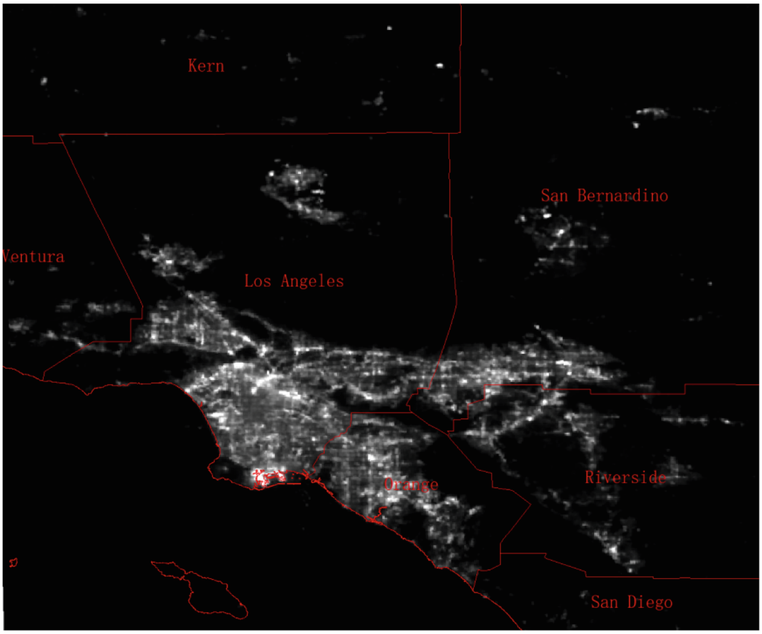

Fig. 3. The VIIRS night-time light image for Los Angeles

2.3 Statistical Analysis

To evaluate the relationship between different datasets, we used Pearson and Spearman's rank correlation analysis. The datasets include the remote sensing images and road network data. The Pearson coefficient is defined as

$$\rho_{XY} = \frac{\mathrm{cov}(X, Y)}{\sigma_X \sigma_Y} \tag{1}$$

where X, Y are two observed vector data of two variable x, y, σ_X and σ_Y are standard deviation of X and Y, and cov(X,Y) is covariance between X and Y.

The Spearman's correlation coefficient is defined as:

$$r_{X,Y} = \frac{\mathrm{cov}(rg_X, rg_Y)}{\sigma_{rg_X} \sigma_{rg_Y}} \tag{2}$$

where $r_{X,Y}$ is the Spearman's correlation coefficient between X and Y, rg_X, rg_Y are the rank number of X and Y, respectively, and σ_{rg_X} and σ_{rg_Y} are the standard variation of rg_X, rg_Y, respectively. While Pearson correlation reflects linear relationship between two variables, Spearman correlation reflects monotonic relationship, including both linear and nonlinear relationship, between two variables.

2.4 Road Network Analysis

It is known that the street light is a major contributor to the night-time light, and the street light has shown a linear feature in the night-time light images [18]. Normally, road intersections are always brighter than the surrounding areas since they have higher density traffic lights, so that the intersections can be viewed as point features in the night-time light images (Fig. 4). We will investigate how the night-time light images are responding to the linear features and point features, and the linear features are the primary road derived from the road network data, and the point features are the primary road intersections. Although there are several types of roads in Los Angeles, we only use the primary roads as our research material since this type of road has highest density lighting which can be effectively recorded by the satellite imagery.

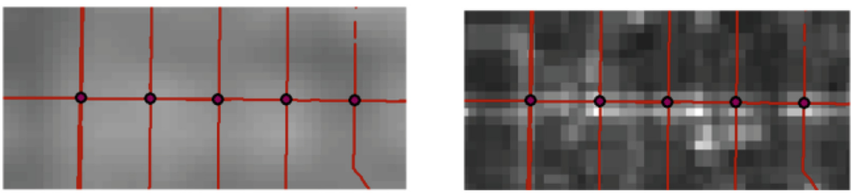

(a) (b)

Fig. 4. A sample image patch overlapped with road network, showing the night-time light response to the primary road and primary road intersections: a) VIIRS and; b) Luojia-1

We employ buffer zone analysis to quantify how night-time light responds to the primary roads: 1) A buffer zone with distance of 500 m to the primary roads is generated. For each pixel in the buffer zone, we calculate its distance to the primary road and record its radiance value from night-time light images; 2) The whole buffer zone in the image is split into several subzones based on the number of the neighborhood areas; 3) For each buffer zone, there are several pixels, and the correlation between the distance and radiance is calculated. We record the correlation coefficient between road distance and Luojia-1 radiance, as well as the correlation coefficient between road distance and VIIRS radiance; 4) we compare the groups of correlation coefficients of both Spearman and Pearson for Luojia-1 and VIIRS.

In addition, we employ a similar way to quantify how night-time light responds to the primary road intersections: 1) Candidates of primary road intersections were extracted from the primary road network. We remove the fake intersections by hand since the topology of the road networks has some mistakes. For the intersections which fall into the same footprint of night-time light pixel (100 m resolution), we only remain one intersection for those intersections; 2) Buffers zones with distance of 500 m to the intersections are generated; 3) For each pixel in a buffer zone, we calculate its distance to the intersection and collect its radiance value from night-time light images of both Luojia-1 and VIIRS; 4) For each buffer zone, we record the correlation coefficient between distance to road intersection and Luojia-1 radiance, and the correlation coefficient between distance to intersection and VIIRS radiance; 5) We compare the groups of correlation coefficients of both Spearman and Pearson for Luojia-1 and VIIRS.

For both the primary roads and primary road intersections which are night-time light sources, the night-time light is regarded to be responding to the road network if the night-time light radiance is negatively correlated to the distance to the primary roads or primary road intersections, because the light sources have a distance-decay effect in spatial dimension.

3 Results

3.1 Visual Evaluation

When we compare the Luojia-1 and VIIRS images by visual evaluation (Figs. 2 and 3), the Luojia-1 image is much clearer than the VIIRS image. The linear features and point features, from the road networks, are apparent in the Luojia-1 image, while those in the VIIRS image are blurry although some of the features are still visible from the VIIRS image. For the linear features, only very bright roads in the Luojia-1 image can be seen in the VIIRS image, while the dim roads in the Luojia-1 image are invisible in the VIIRS image. However, this is only qualitative comparison, and the quantitative analysis will be carried out in rest of this section.

3.2 Night-Time Light Response to Primary Roads

We calculated the correlation coefficient between the image radiance and distance to the primary road in the buffer zone of each neighborhood area. For each neighborhood, we have a correlation coefficient value for each kind of image. Since some neighborhood areas have very little length of primary roads, they have very few pixels in the buffer zones. We excluded these neighborhood areas with area smaller than 600 m^2 (equal to 6 pixels at 100 m resolution), and finally we got 228 neighborhood areas for analysis. The Spearman correlation coefficients are shown in Fig. 5. For both the Luojia-1 image and VIIRS image, the image radiance is negatively correlated to the distance to the primary roads for most of the neighborhood areas ($p < 0.01$). In addition, the Luojia-1 image radiance is more negatively correlated to the distance to the primary roads than that of the VIIRS image, as shown in Fig. 5. These finding can be proved by quantitative evaluation in Tables 1 and 2.

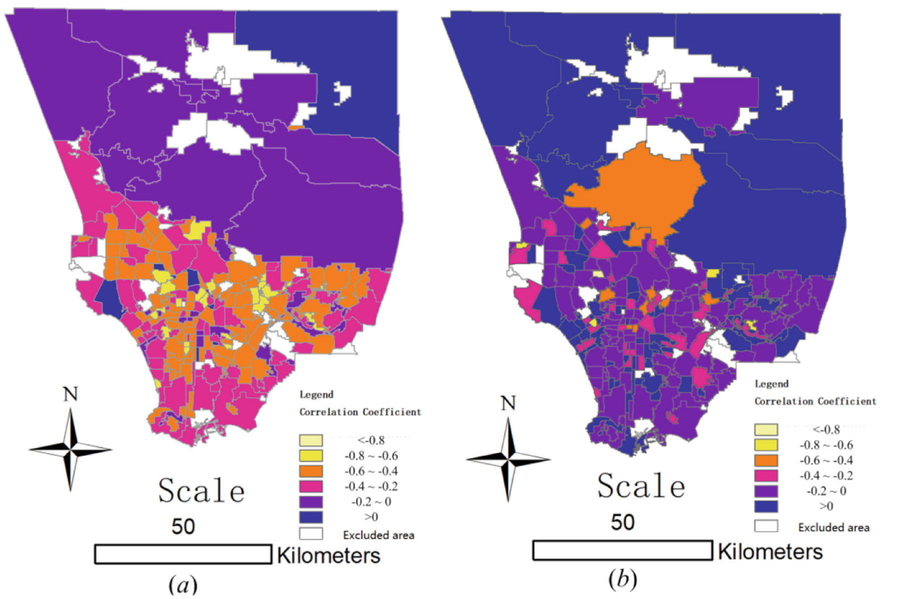

Fig. 5. The correlation coefficient (Spearman) between night-time light and distance to the primary road: (a) Luojia-1 image; (b) VIIRS image

For the Spearman correlation, 217 out of the 228 neighborhood areas have negative values of the correlation for Luojia-1 image ($p < 0.01$), while that of the VIIRS is only 161 ($p < 0.01$). As we change the threshold to smaller ones, from 0 to −0.5, we can see the contrast more obviously: 45 neighborhood areas have correlation coefficient smaller than −0.5 for Luojia-1 image, while that of the VIIRS image is only 8. The average correlation coefficient for Luojia-1 and VIIRS images are −0.3193 and −0.0915, respectively, also suggesting the correlation coefficient of Luojia-1 is much more negative than that of the VIIRS. In addition, we list the Pearson correlation results in

Table 1. Distribution of Spearman correlation coefficients (N = 228) between the radiance of night-time light images and the distance to the primary road

Sensor	Number of neighborhood areas	Number of neighborhood areas with correlation coefficient (c) less than a threshold				Mean value of the correlation coefficient
		$c < 0$	$c < -0.1$	$c < -0.3$	$c < -0.5$	
Luojia-1	228	220	212	152	70	−0.3843
VIIRS	228	157	117	27	10	−0.0974

Table 2. Distribution of Pearson correlation coefficients between the radiance of night-time light images and the distance to the primary road

Sensor	Number of neighborhood areas	Number of neighborhood areas with correlation coefficient (c) less than a threshold				Mean value of the correlation coefficient
		$c < 0$	$c < -0.1$	$c < -0.3$	$c < -0.5$	
Luojia-1	228	217	198	125	45	−0.3193
VIIRS	228	161	113	26	8	−0.0915

Table 2, which have the same pattern to the Table 1, and the only difference is the Pearson correlation is weaker than the Spearman correlation.

3.3 Night-Time Light Response to Primary Road Intersections

484 primary road intersections were selected. We calculated the correlation coefficients between image radiance and distance to the intersections in the buffer zones. Since some buffer zones are overlapped, it is complicated to show the results in a map, thus we only list the statistical results in Tables 3 and 4. From Table 3 of Spearman correlation, 431 out of 484 neighborhood areas have negative correlation coefficient for Luojia-1, and the number is 350 for VIIRS ($p < 0.01$). As we gradually move the threshold from 0 to −0.5, the contrast becomes larger: 111 out of 484 neighborhood areas have correlation coefficient less than −0.5 for Luojia-1, and the number is 34 for VIIRS. The average coefficient for Luojia-1 is −0.3129 and that of the VIIRS is −0.1370.

From Table 4 of Pearson correlation, 399 neighborhood areas have negative value of correlation coefficient for Luojia-1, while the number is 316 for VIIRS. The general pattern revealed by Table 4 is similar to that of Table 3. Both the Tables 3 and 4 indicate the image radiance of Luojia-1 is more strongly correlated to the road intersections than that of the VIIRS. In other words, the Luojia-1 image is more responsive to road intersection than the VIIRS image.

Table 3. Distribution of Spearman correlation coefficients between the radiance of night-time light images and the distance to the primary road intersections

Sensor	Number of neighborhood areas	Number of neighborhood areas with correlation coefficient (c) less than a threshold				Average correlation coefficient
		c < 0	c < −0.1	c < −0.3	c < −0.5	
Luojia-1	484	431	387	269	111	−0.3129
VIIRS	484	350	266	109	34	−0.1370

Table 4. Distribution of Pearson correlation coefficients between the radiance of night-time light images and the distance to the primary road intersections

Sensor	Number of neighborhood areas	Number of neighborhood areas with correlation coefficient (c) less than a threshold				Average correlation coefficient
		$c < 0$	$c < -0.1$	$c < -0.3$	$c < -0.5$	
Luojia-1	484	399	357	249	128	−0.2967
VIIRS	484	316	232	98	33	−0.1100

4 Conclusions

To evaluate the Luojia-1 image with some ground truth knowledge, the road network analysis was used. The basic assumption of the analysis is the night-time light along the road should have a distance-decay effect, so that the correlation analysis can help to quantify how much the night-time light responds to the night-time light sources. We found that the coefficient values from both the Spearson and Spearman correlation analysis for Luojia-1 image are not high, at an average value about 0.3, although much higher than those of the VIIRS image. This phenomenon occurs because there are many types of buildings such as shops, churches and gas stations along the roads, and these buildings also emitted light at night [18]. Therefore, the radiance does not well follow the distance-decay pattern, but is only correlated to the distance to the roads and road intersections. This study supports the previous study that Luojia-1 has more spatial details than VIIRS when the wavelet energy is used as the measurement. In summary, Luojia-1 images can provide more spatial details than the VIIRS images, suggesting that urban structures can be better analyzed with the Luojia-1 dataset.

Acknowledgements. This research was supported by Youth Fund of Wuhan Donghu University under grant no. 2018dhsk004 and Open Fund of State Laboratory of Information Engineering in Surveying, Mapping and Remote Sensing, Wuhan University, under grant no. 18T06.

References

1. Croft, T.A.: Burning waste gas in oil fields. Nature **245**(5425), 375–376 (1973)
2. Croft, T.A.: Nighttime images of the earth from space. Sci. Am. **239**, 86–98 (1978)
3. Welch, R.: Monitoring urban population and energy utilization patterns from satellite data. Remote Sens. Environ. **9**(1), 1–9 (1980)
4. Elvidge, C.D., Baugh, K.E., Kihn, E.A., Kroehl, H.W., Davis, E.R., Davis, C.W.: Relation between satellite observed visible-near infrared emissions, population, economic activity and electric power consumption. Int. J. Remote Sens. **18**(6), 1373–1379 (1997)
5. Sutton, P.: Modeling population density with night-time satellite imagery and GIS. Comput. Environ. Urban Syst. **21**(3), 227–244 (1997)
6. Henderson, M., Yeh, E.T., Gong, P., Elvidge, C., Baugh, K.: Validation of urban boundaries derived from global night-time satellite imagery. Int. J. Remote Sens. **24**(3), 595–609 (2003)
7. Small, C., Pozzi, F., Elvidge, C.D.: Spatial analysis of global urban extent from DMSP-OLS night lights. Remote Sens. Environ. **96**(3–4), 277–291 (2005)
8. Zhang, Q., Seto, K.: Mapping urbanization dynamics at regional and global scales using multi-temporal DMSP/OLS nighttime light data. Remote Sens. Environ. **115**(9), 2320–2329 (2011)
9. Huang, Q., et al.: Detecting the 20 year city-size dynamics in China with a rank clock approach and DMSP/OLS nighttime data. Landscape Urban Plan. **137**, 138–148 (2015)
10. Wei, Y., Liu, H., Song, W., Yu, B., Xiu, C.: Normalization of time series DMSP-OLS nighttime light images for urban growth analysis with Pseudo Invariant Features. Landscape Urban Plan. **128**, 1–13 (2014)
11. Henderson, J.V., Storeygard, A., Weil, D.N.: Measuring economic growth from outer space. Am. Econ. Rev. **102**(2), 994–1028 (2012)
12. Li, X., Li, D.: Can night-time light images play a role in evaluating the Syrian Crisis? Int. J. Remote Sens. **35**(18), 6648–6661 (2014)
13. Bennie, J., Davies, T.W., Duffy, J.P., Inger, R., Gaston, K.J.: Contrasting trends in light pollution across Europe based on satellite observed night time lights. Sci. Rep. **4** (2014). Article number: 3789
14. Elvidge, C.D., Baugh, K.E., Zhizhin, M., Hsu, F.C.: Why VIIRS data are superior to DMSP for mapping nighttime lights. Proc. Asia-Pacific Adv. Netw. **35**, 62–69 (2013)
15. Li, X., et al.: Anisotropic characteristic of artificial light at night – systematic investigation with VIIRS DNB multi-temporal observations. Remote Sens. Environ. **233**, 111357 (2019)
16. Li, X., Li, X., Li, D., He, X., Jendryke, M.: A preliminary investigation of Luojia-1 night-time light imagery. Remote Sens. Lett. **10**(6), 526–535 (2019)
17. Li, X., Zhao, L., Li, D., Xu, H.: Mapping urban extent using Luojia 1-01 nighttime light imagery. Sensors **18**(11), 3665 (2018)
18. Kuechly, H.U., et al.: Aerial survey and spatial analysis of sources of light pollution in Berlin, Germany. Remote Sens. Environ. **126**, 39–50 (2012)